scilight

23-Hydroxybetulinic Acid, A Natural Compound, Alleviates DSS-induced Colitis by Regulating NF-κB Signaling

Shuangli Xiang [1,#], Miaojuan Wang [2,#], and Xiuping Chen [2,*]

[1] Key Laboratory of Basic Pharmacology of Ministry of Education and Joint International Research Laboratory of Ethnomedicine of Ministry of Education, Zunyi Medical University, Zunyi 400804, China.
[2] State Key Laboratory of Quality Research in Chinese Medicine, Institute of Chinese Medical Sciences, University of Macau, Macao, China.
* Correspondence: xpchen@um.edu.mo, Tel.: +853-88224679, Fax: +853-28841358
# Co-First author.

Abstract: Ulcerative colitis (UC), an inflammatory intestinal disease, is a growing epidemic affecting people worldwide and requires the development of effective therapeutic drugs. In this study, the effect of 23-hydroxybetulinic acid (23-HBA), a compound isolated from the traditional herb *Pulsatilla chinensis* (Bunge) Regel, on experimental UC was studied. C57BL/6J male mice were administrated with 3% dextran sodium sulfate (DSS) in drinking water to establish the UC model. 23-HBA was orally administrated at either 3.75, 7.5, or 15 mg/kg for 6 days. Mesalazine was used as a positive control. Examination of the body weight, colon length, disease activity index (DAI), histopathology examination, inflammatory cytokines, oxidative stress, and protein expression was performed. The pathological changes were examined with hematoxylin and eosin (H&E) and Aixian blue-glycogen (AB-PAS) staining. In cultured RAW 264.7 cells, the effects of 23-HBA on lipopolysaccharide (LPS)-stimulated cyclooxygenase-2 (COX-2), inducible nitric oxide synthase (iNOS), and oxidative stress were analyzed. Compared with the colitis model, 23-HBA treatment significantly increased the body weight and colon length and decreased the DAI score. Pathological staining showed that 23-HBA mitigated the damage in intestinal structures, the increase in inflammatory cell infiltration, the increase in submucosa edema, and the decrease in goblet cell number. Furthermore, 23-HBA decreased IL-1β, IL-6, and MDA levels in the colon tissues. In addition, 23-HBA inhibited the protein expressions of COX-2, iNOS, and NF-κB p65 both in the colon tissues and in LPS-stimulated RAW 264.7 cells. In conclusion, these results showed that 23-HBA alleviated DSS-induced acute UC in mice and inhibited LPS-stimulated inflammation in RAW 264.7 cells possibly mediated by regulating the NF-κB pathway.

Keywords: 23-Hydroxybetulinic acid; dextran sodium sulfate; ulcerative colitis; inflammation

1. Introduction

Ulcerative colitis (UC) is a non-specific inflammatory disease of the intestine. The worldwide incidence of UC is increasing in recent years [1]. Although the incidence of UC in Asia is relatively low, it is rising significantly [2,3]. The typical clinical symptoms include abdominal pain, diarrhea, and blood in the stool [4]. Accumulated data revealed that the inflammatory response of UC is limited to the mucosal surface and the main pathological manifestations are intestinal barrier destruction, crypts disappearance or abscesses, deformation of mucosal glands, inflammatory cells infiltration and goblet cells loss [4-6]. Though there are several categories of drugs available for UC treatment, their undesired side effects and the high risk of carcinogenesis of UC call for novel therapeutic strategies.

Pulsatilla chinensis (Bunge) Regel (Baitouweng, BTW), the dried root of Chinese Pulsatilla is a widely used traditional herb in Traditional Chinese Medicine (TCM). In TCM theory, BTW has the effects of heat-clearing, detoxifying and blood-cooling (Qingren Jiedu Liangxue). It is the monarch in a four-herb prescription termed BTW decoction which demonstrates a beneficial effect in numerous clinical practices [7–9]. However, the specific material basis of BTW remains unclear.

23-Hydroxybetulinic acid (23-HBA) is one of the major chemical components of BTW, accounting for 1.26–1.53% [10]. However, only a few studies demonstrated its anti-cancer [11,12] and cardioprotective effects [13]. Anemoside B4 (AB4), another compound isolated from BTW, was reported to have a beneficial effect on UC by suppressing toll-like receptor 4 (TLR4)/nuclear factor kappa B (NF-κB)/mitogen-activated protein kinase (MAPK) pathway [14]. Interestingly, a metabolic study showed that 23-HBA may be the metabolite of AB4 and may mediate the anti-inflammatory and immune-regulating roles of AB4 [10]. However, there is limited data regarding the regulatory effect and mechanism of 23-HBA on inflammation. Here, we determined the effect and the underlying mechanism of 23-HBA using dextran sodium sulfate (DSS) -induced UC mice and lipopolysaccharide (LPS) -stimulated RAW 264.7 cells.

2. Materials and Methods

2.1. Chemicals and Reagents

23-HBA (≥98%) was purchased from Baoji Herbest Bio-Tech Co., Ltd (Baoji, China). Mesalazine was purchased from Beijing Bailingwei Technology Co., Ltd (Beijing, China). DSS was supplied by MP Biomedicals. LPS, Griess reagent, and TLR4 antibodies were obtained from Beyotime (Shanghai, China). Malondialdehyde (MDA), myeloperoxidase (MPO), and superoxide dismutase (SOD) assay kits and Aixian blue-glycogen (AB-PAS) staining solution was obtained from Nanjing Jiancheng Technology Co., Ltd (Nanjing, China). DCFH$_2$-DA was obtained from Sigma-Aldrich (St Louis, USA). The ELISA kits for IL-1β, IL-6, IL-10, and prostaglandin E2 (PEG2) were provided by Elabscience Biotechnology Co., Ltd. (Wuhan, China) and Mlbio (Shanghai, China), respectively. Antibodies for NF- κB p65 (p65), phosphorylated NF- κB p65 (Ser536) (p-p65), p-IKKα/β, IKKα, IKKβ, p-IκBα, and IκBα were obtained from Cell Signaling Technology (Beverly, USA). COX-2 antibody was provided by Abcam (Cambridge, UK). Antibodies for beta-actin, iNOS, MyD88, and GAPDH were purchased from Proteintech Group, Inc (Wuhan, China).

2.2. Cell Culture

RAW 264.7 cell line was obtained from ATCC (Manassas, USA). Cells were cultured in DMEM supplemented with 10% FBS and 1% penicillin-streptomycin solution in a humidified atmosphere of 5% CO$_2$ at 37°C.

2.3. Animal Model

6 weeks old male C57BL/6 mice were supplied by Beijing HFK Bio-Technology Co., Ltd (Beijing, China) and were kept in SPF animal facilities. The DSS-induced UC model was established in our previous report [15]. Briefly, 36 mice were randomly divided into six groups (n=6): control group, model (3% DSS) group, mesalazine (150 mg/kg) group, and 3% DSS + 23-HBA-L (3.75 mg/kg)/23-HBA-M (7.5 mg/kg)/23-HBA-H (15 mg/kg) groups. The 23-HBA dosages were chosen according to preliminary experimental results. Mesalazine, the first-line drug for patients with mild to moderate UC, was chosen as the positive control. 23-HBA or mesalazine was orally administrated daily for 6 days (one day after the DSS challenge). DSS was dissolved in drinking water and replaced every day for 7 days. On day 8, mice were sacrificed and samples of colon tissues and serum were collected. The animal experiment was approved by the Animal Ethics Committee of Zunyi Medical University (ZMU21-2208-009).

2.4. Calculation of Disease Activity Index (DAI) Score

Weight loss, stool consistency, intestinal bleeding, etc were daily recorded for 7 days. The DAI score

was calculated as previously reported [15].

2.5. Hematoxylin and Eosin (H&E) and AB-PAS Staining

The collected colon tissues were embedded into paraffin sections by conventional methods. The hematoxylin and eosin (H&E) for general pathological observation and AB-PAS stainings for goblet cells were performed as in our previous reports [16,17]. The sections were observed using the Olympus BX43+ DP2b Optional Microscope (Tokyo, Japan) and images were obtained.

2.6. Immunohistochemical Staining for Protein Expression

The colon tissue paraffin slices were dewaxed and heat-induced antigen retrieved. Then they were treated with endogenous peroxidase blocker for 15 min in the dark. The sections were incubated with antibodies of COX2 (1:100), iNOS (1:50), NF-κB p65 (1:50), and NF-κB p-p65 (1:50), respectively. Then the slides were washed with PBS and incubated with anti-rabbit secondary antibodies at 37°C for 20 min. After adding the horseradish enzyme-labeled streptavidin and incubating it at 37°C for 20 min, the color reaction was developed with 3,3-diaminobenzidine tetrahydrochloride.

2.7. Immunofluorescence Staining for NF-κB p65

The colon tissue slices were permeabilized with 0.3% Triton X-100 at room temperature for 3 hours and then blocked with goat serum for 1 hour. Immunofluorescence staining was performed by using antibodies of NF-κB p65 (1:50) and NF-κB p-p65 (1:50) carried with CoraLite488-conjugated secondary antibody. The nuclear was stained with DAPI. Images were obtained using the Olympus BX53+DP80 Upright Fluorescence Microscope (Tokyo, Japan).

2.8. ELISA Assays for IL-1β, IL-6, IL-10, and PGE2

The levels of IL-1β, IL-6, and IL-10 in the colon tissues were quantitatively analyzed with ELISA kits following the manufacturer's protocols. RAW 264.7 cells were treated with different concentrations (2.5–10 μM) of 23-HBA for 1 hour followed by LPS (1 μg/mL) stimulation for 18 hours. The secretion of PGE2 in the culture medium was detected with an ELISA kit following the manufacturer's protocol.

2.9. Determination of MDA, MPO, and SOD

The MDA content and MPO activity in the colon tissues were tested with commercial kits according to the manufacturer's protocols. The SOD activity in serum was examined using a kit following the manufacturer's protocol.

2.10. Nitrite Content Assay

RAW264.7 cells were treated with different concentrations (2.5–10 μM) of 23-HBA for 1 hour and then stimulated with LPS (1 μg/mL) for 18 hours. The culture medium was collected and the nitrite content was determined with Greiss Reagent as in our previous report [18].

2.11. Western Blotting for Protein Expression

Total proteins from the colon tissues and RAW264.7 cells were extracted and the protein content of each sample was determined by the BCA kit. Proteins were separated with 8% sodium dodecyl-sulfate polyacrylamide gel electrophoresis (SDS-PAGE) and transferred to polyvinylidene fluoride (PVDF) membranes. After being blocked with 5% non-fat milk for 2 hours at room temperature, the membranes were then incubated with specific antibodies (COX-2, iNOS, TLR4, p-IKKα/β, p-IκBα, p65, p-p65, MyD88, GAPDH, β-actin) at 4°C overnight. Then membranes were washed with Tris-buffered saline with Tween 20 (TBST) 3 times and were incubated with the secondary antibody for 1 hour. After incubation with the ECL luminescent solution, images were obtained from the chemiluminescence gel imaging system (Bio-Rad, USA). The western blotting results were analyzed using Image-Lab 6.0 software.

2.12. Determine the Intracellular Reactive Oxygen Species (ROS)

RAW264.7 cells were treated with different concentrations (2.5–10 μM) of 23-HBA for 1 hour followed by LPS (1 μg/mL) stimulation for 4 hours. The ROS levels were determined by fluorescent probe DCFH$_2$-DA (10 μM) using a FACScan™ flow cytometer (BD Biosciences).

2.13. Statistical Analysis

Results were presented as mean ± SD. SPSS 18.0 was used to perform the statistical analyses with one-way ANOVA and the *t*-test was used to compare the differences between the two groups. A *p* < 0.05 was regarded as a statistical difference.

3. Results

3.1. 23-HBA Alleviated Acute UC

Compared with mice in the control group, the mice's body weights in the model group were significantly decreased. Both 23-HBA and mesalazine treatment significantly inhibited body weight loss (Figure 1A). The DAI scores increased in the model group and 23-HBA and mesalazine treatment significantly decreased the DAI score from day 5 (Figure 1B). In addition, DSS-induced significant contract of colonic tissues. Compared with mice in the model group, the colon length and weight in 23-HBA and mesalazine-treated groups were increased (Figures 1C–1E).
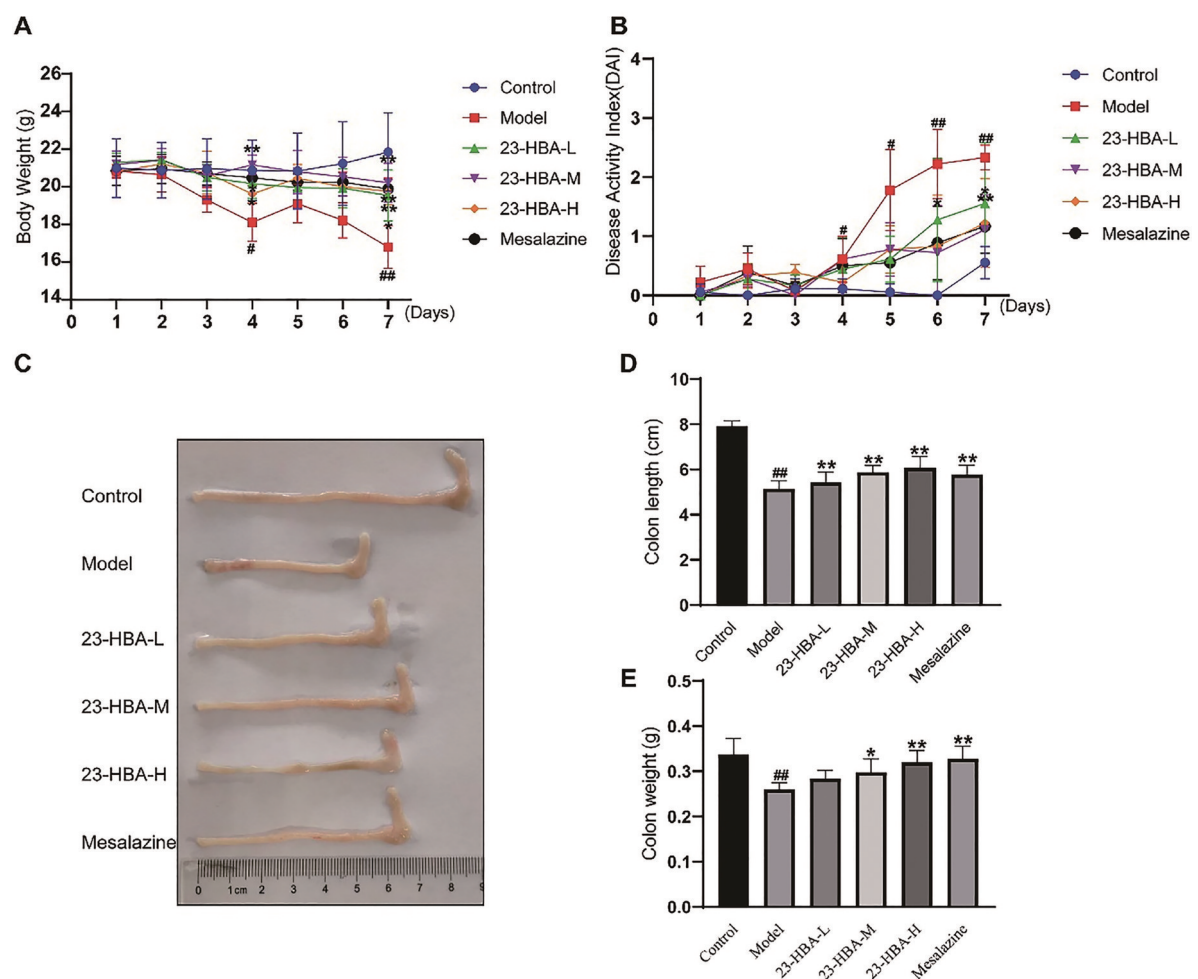

Figure 1. 23-HBA mitigated DSS-induced acute colitis in mice. The effect of 23-HBA on body weight (**A**), DAI (**B**), disease activity index (**C**), colon length (**D**), and colon weight (**E**) was determined and calculated. *p* < 0.05, **p* < 0.01 vs model; #*p* < 0.05, ##*p* < 0.01 vs control. 23-HBA-L (3.75 mg/kg), 23-HBA-M (7.5 mg/kg), 23-HBA-H (15 mg/kg).

3.2. 23-HBA Mitigated the Pathological Injuries

H&E staining results showed that the colon tissues of the control mice were structurally intact. The mucosal layer cells were morphologically intact and the crypts were well-arranged. There was no inflammatory cell infiltration and no loss of intestinal epithelial cells. In contrast, the colon tissues in model mice were severely injured as evidenced by necrotic mucosal cells, a large number of inflammatory cell infiltration, submucosa edema, disappearance of crypts and gland structures. These changes in colon tissues were significantly inhibited by 23-HBA administration, especially in the high-dosage group (Figure 2A). AB-PAS staining revealed that the goblet number in the mice of the model group was reduced, which was dose-dependently improved by 23-HBA (Figure 2B).
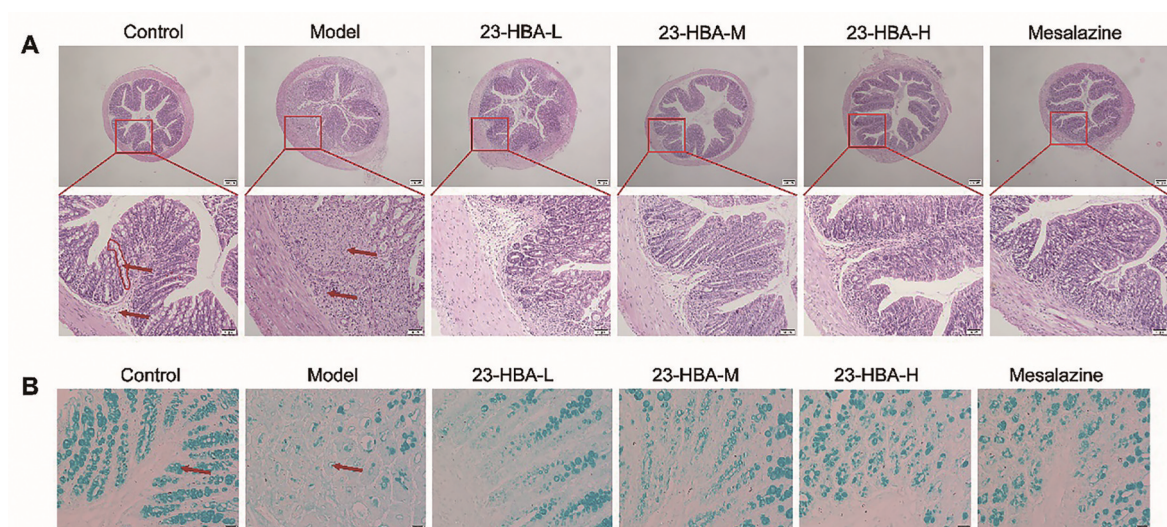

Figure 2. 23-HBA ameliorated histopathological changes of DSS-induced acute colitis in mice. (**A**) H&E staining of colon tissues (magnification 40× and 200×, scale bar: 200 μm and 50 μm. red circle: crypt; red arrow: mucosal layer and submucosa). (**B**) AB-PAS staining for goblet cells (magnification 400 ×, scale bar: 20 μm. red arrow: goblet cells). 23-HBA-L (3.75 mg/kg), 23-HBA-M (7.5 mg/kg), 23-HBA-H (15 mg/kg).

3.3. 23-HBA Reduced COX-2, iNOS, PEG2, and Nitrite Levels

To explore the underlying mechanism of 23-HBA, its anti-inflammatory effect was tested using cellular assays. 23-HBA treatment significantly inhibited LPS-induced protein expression of COX-2 in RAW264.7 cells and decreased LPS-induced secretion of PGE2 in the culture medium (Figures 3A and 3B). Western blotting results indicated that COX-2 expression in colon tissues was significantly increased in the model mice, which was inhibited by both 23-HBA and mesalazine (Figure 3C). Immunohistochemical staining results showed intensive brown signals in model mice indicating high expression of COX-2. In contrast, expression signals in both 23-HBA and mesalazine-treated groups were significantly decreased (Figure 3D).

23-HBA significantly inhibited LPS-induced protein expression of iNOS in RAW264.7 cells and decreased the levels of nitrite in the culture medium (Figures 4A and 4B). Western blotting results indicated that the iNOS expression in colon tissues was significantly increased in the model mice, which was inhibited by both 23-HBA and mesalazine treatment (Figure 4C). Immunohistochemical staining results showed intensive brown signals in model mice indicating high expression of iNOS. In contrast, the expression of iNOS in both 23-HBA and mesalazine-treated groups was significantly decreased (Figure 4D).

3.4. 23-HBA Inhibited the Generation of Pro-inflammatory Cytokines and Oxidative Stress

Compared with the control group, the levels of IL-1β and IL-6 in colon tissues were significantly increased while the IL-10 level was decreased in the mice of the model group (Figures 5A – 5C). Both 23-HBA and
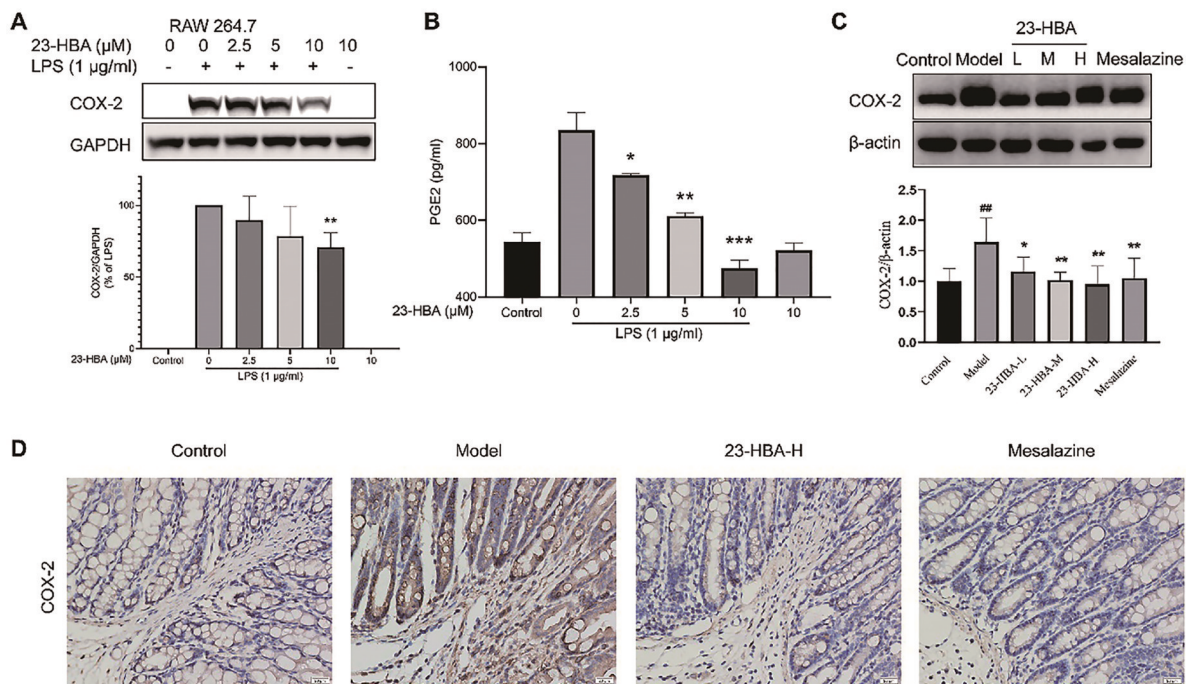
Figure 3. 23-HBA reduced COX-2 expression in LPS-stimulated Raw264.7 cells and colon tissues of acute colitis in mice. Effect of 23-HBA on LPS-induced COX-2 expression (**A**) and PEG$_2$ secretion (**B**) in RAW264.7 cells. The effect of 23-HBA on COX-2 expression in colon tissues was determined by western blotting (**C**) and immunohistochemistry (**D**) (magnification 400 ×, scale bar: 20 μm). The data were presented as the mean ± SD. *$p < 0.05$, **$p < 0.01$, ***$p < 0.005$ vs model; ##$p < 0.01$ vs control. 23-HBA-L (3.75 mg/kg), 23-HBA-M (7.5 mg/kg), 23-HBA-H (15 mg/kg).
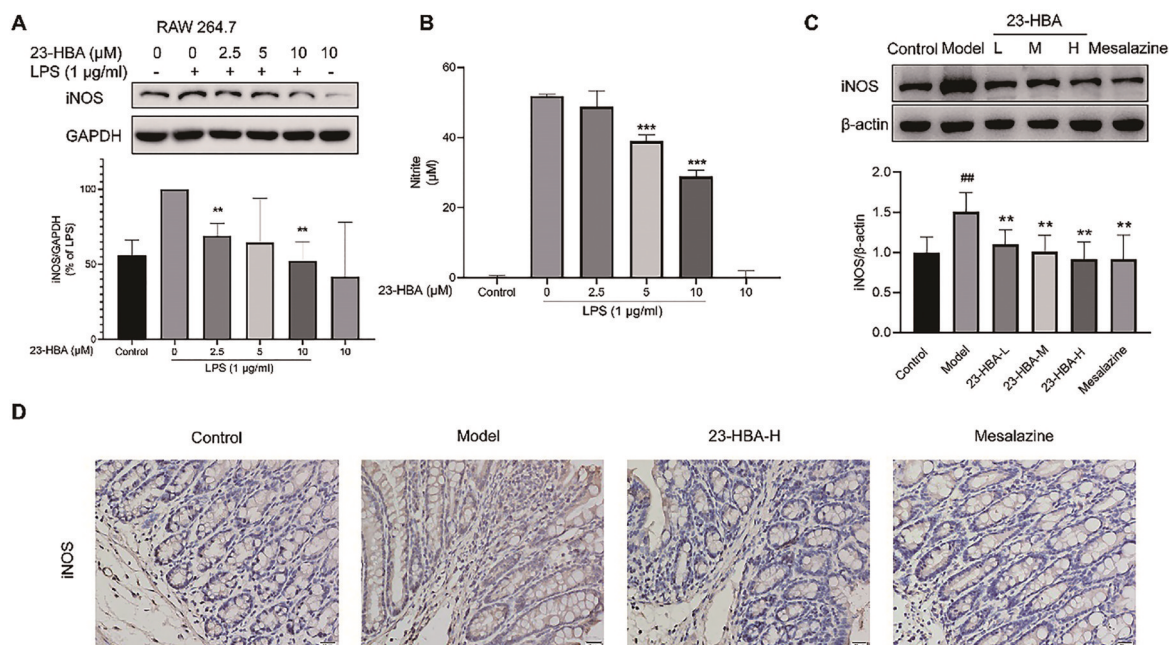

Figure 4. 23-HBA reduced iNOS expression in LPS-stimulated Raw 264.7 cells and colon tissues of acute colitis in mice. Effect of 23-HBA on LPS-induced iNOS expression (**A**) and nitrite levels (**B**) in RAW 264.7 cells. The effect of 23-HBA on iNOS expression in colon tissues was determined by western blotting (**C**) and immunohistochemistry (**D**) (magnification 400 ×, scale bar: 20 μm). ***$p < 0.005$, **$p < 0.01$, *$p < 0.05$ vs model; ##$p < 0.01$ vs control. 23-HBA-L (3.75 mg/kg), 23-HBA-M (7.5 mg/kg), 23-HBA-H (15 mg/kg).

mesalazine treatment significantly decreased levels of IL-1β and IL-6 but increased IL-10 levels simultaneously.

Compared with the control group, the MDA content and the MPO activity were increased in the mice of the model group while the serum SOD activity was significantly decreased. Both 23-HBA and mesalazine treatment significantly decreased MDA and MPO but increased SOD, simultaneously (Figures 5D−5F). In addition, LSP stimulated a significant increase in ROS generation in RAW 264.7 cells. 23-HBA treatment significantly decreased LPS-induced intracellular ROS formation (Figure 5G).
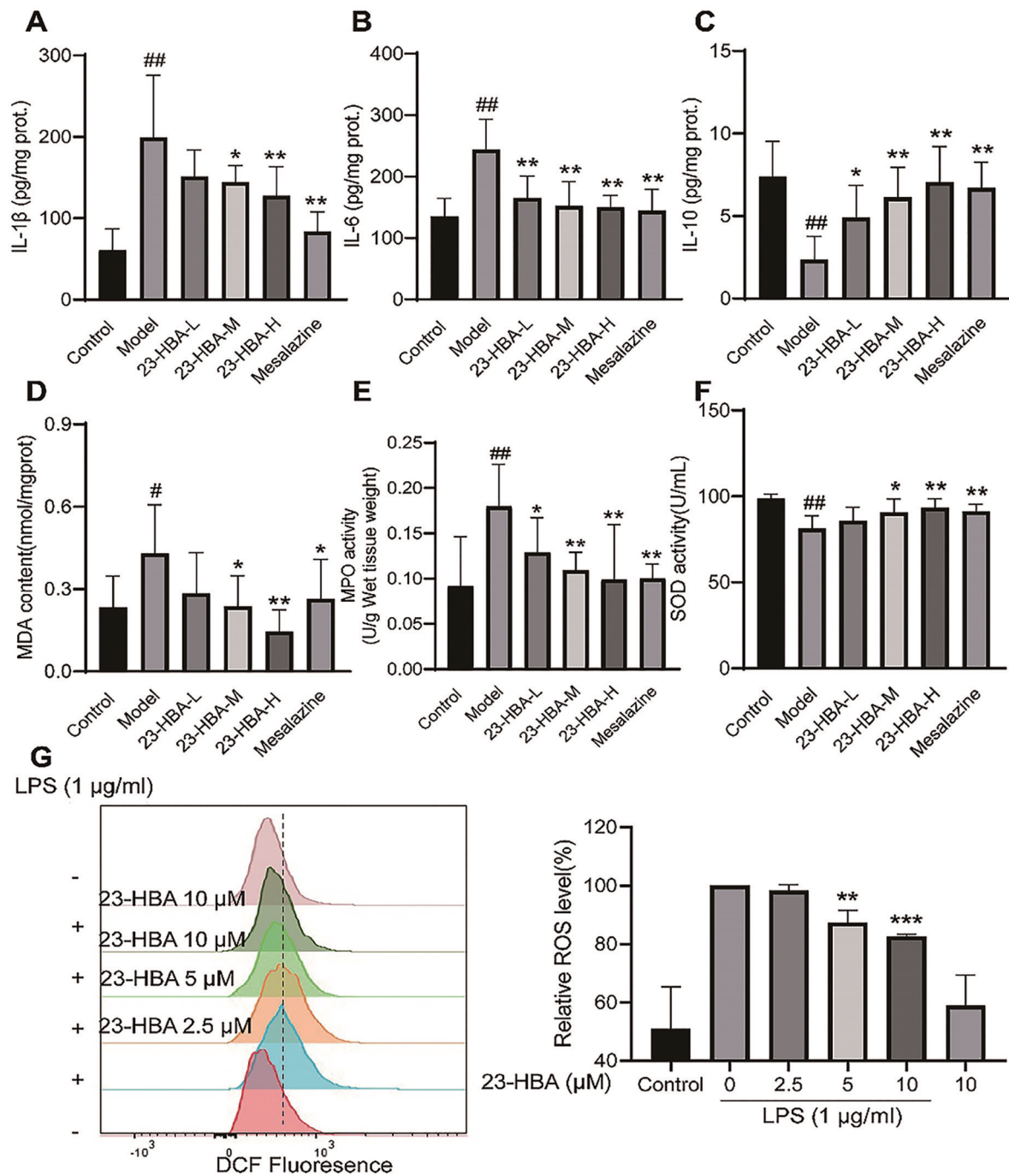

Figure 5. 23-HBA inhibited inflammatory cytokines and oxidative stress. The levels of IL-1β, IL-6, and IL-10 in colon tissues were measured by ELISA (**A−C**). The MDA contents and MPO activity of MPO in colon tissues, and SOD activity in serum (**D−F**) were determined by commercial kits. The effect of 23-HBA on LPS-induced ROS levels in RAW264.7 cells was determined by DCFH$_2$-DA (**G**). *$p < 0.05$, **$p < 0.01$, ***$p < 0.005$ vs model; #$p < 0.05$, ##$p < 0.01$ vs control. 23-HBA-L (3.75 mg/kg), 23-HBA-M (7.5 mg/kg), 23-HBA-H (15 mg/kg). + mean with HBA treatment, - means without HBA treatment.

3.5. 23-HBA Inhibited TLR4 and NF-κB p65 Expression

As shown in Figures 6A-6D, LPS-induced protein expression of TLR4, p-IKKα/β, p-IκBα, and p-p65 in RAW 264.7 cells was significantly suppressed by 23-HBA co-treatment. The protein expression of MyD88, p65, and p-p65 in colon tissues was increased in the model mice, which were significantly inhibited by 3.6. 23-HBA and Mesalazine (Figures 6E–6G).
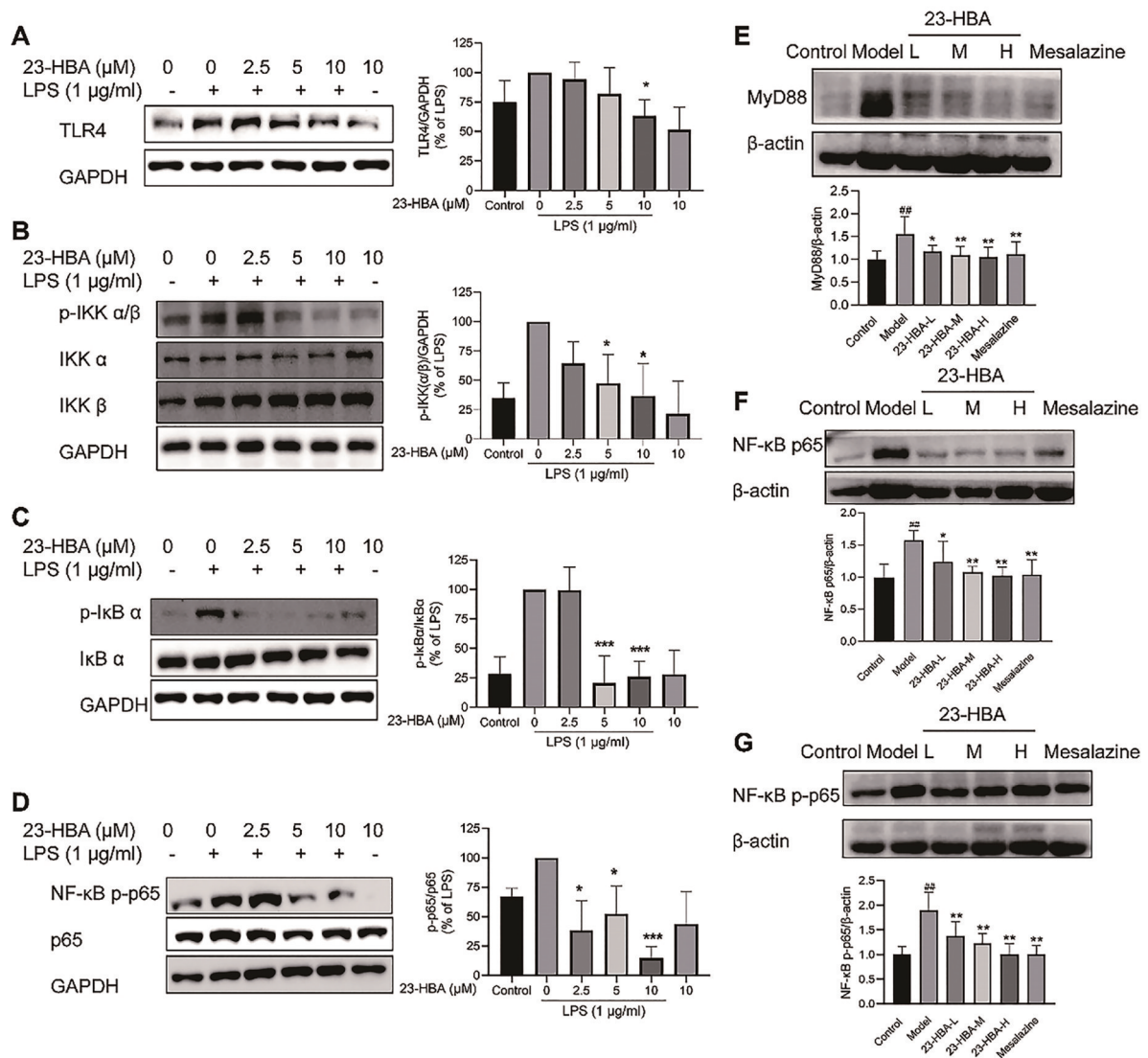

Figure 6. 23-HBA inhibited TLR4 and NF-κB signaling. The effect of 23-HBA on LPS-induced expression of TLR4 (**A**), and p-IKKα/β (**B**), p-IκBα (**C**), and NF-κB p-p65 (**D**) in RAW264.7 cells was determined by Western blotting. Protein expression of MyD88 (**E**), NF-κB p65 (**F**), and p-NF-κB p65 (**G**) in colon tissues. *$p < 0.05$, **$p < 0.01$, ***$p < 0.005$ vs model; ##$p < 0.01$ vs control. 23-HBA-L (3.75 mg/kg), 23-HBA-M (7.5 mg/kg), 23-HBA-H (15 mg/kg).

Immunohistochemical staining results showed intensive brown signals in the model mice indicating high expression of NF‑κB p65 and NF‑κB p-p65. The expression signals in both 23-HBA and mesalazine-treated groups were significantly decreased indicating the expression of NF-κB p65 and NF‑κB p-p65 was inhibited (Figure 7A). Immunofluorescence staining results demonstrated intensive green fluorescence in model mice indicating high expression of NF‑κB p65 and NF‑κB p-p65. The green fluorescence in both 23-HBA and mesalazine-treated groups was significantly decreased indicating the decreased expression of NF-κB p65 and NF‑κB p-p65 (Figures 7B, 7C).
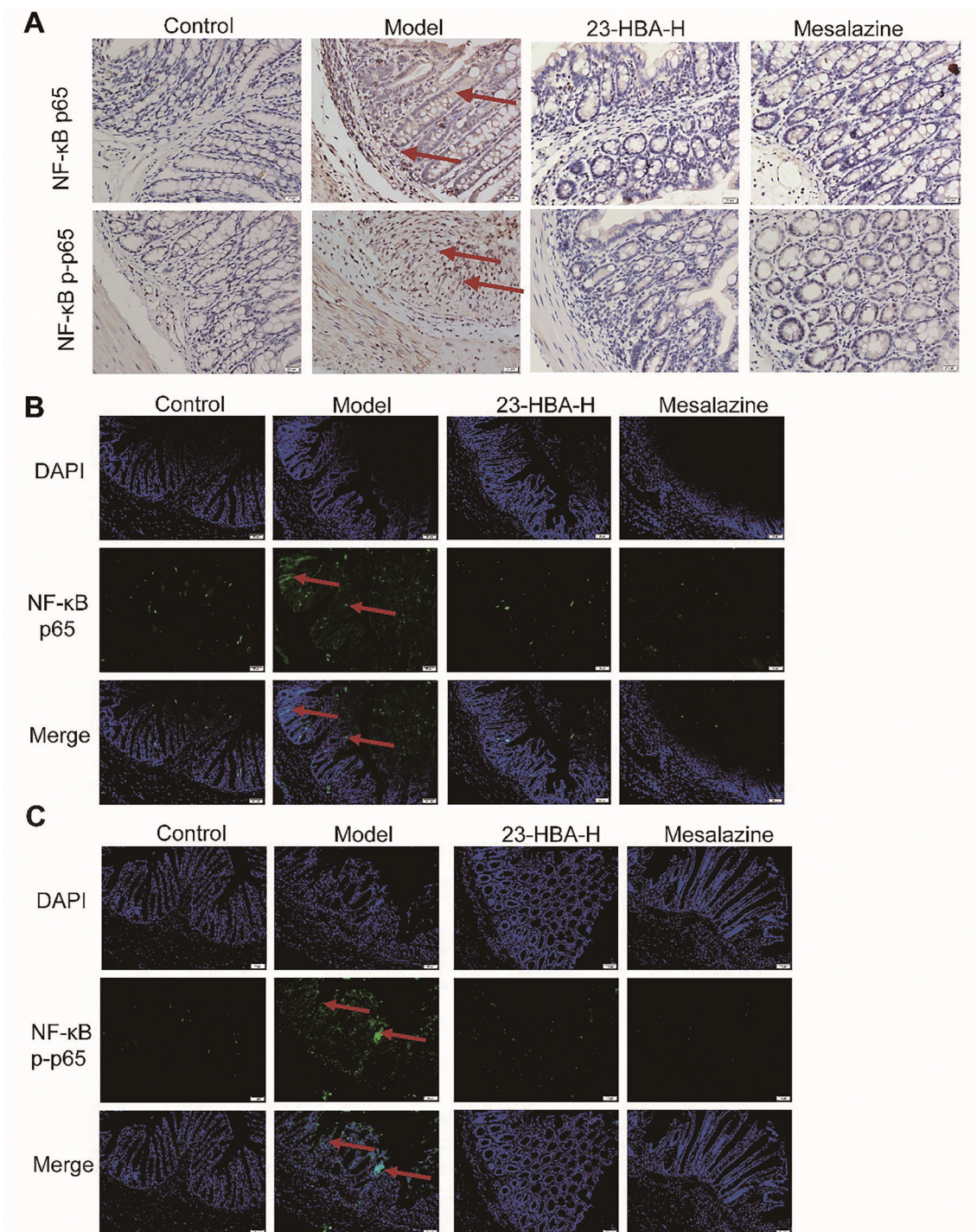
Figure 7. 23-HBA reduced NF-κB p65 and p-p65 expression. (**A**) The effect of 23-HBA on NF-κB p65 and NF-κB p-p65 expressions in colon tissues was determined by immunohistochemistry (**A**) (magnification 400 ×, scale bar: 20 μm) and immunofluorescence (**B**) (magnification 200×, scale bar: 50 μm). 23-HBA-L (3.75 mg/kg), 23-HBA-M (7.5 mg/kg), 23-HBA-H (15 mg/kg). Red arrows, expression of p65 and p-p65.

4. Discussion

The incidence of UC is increasing in both developing and developed countries. Various UC models have been developed to investigate the pathogenesis of UC and drug evaluation. The DSS-induced UC model is a simple and economic tool for UC studies [19,20]. DSS insults induce decreased body weight, increased DAI,

shortened colon length, diarrhea, and blood in stool in mice. H&E and AB-PAS staining showed severe damage in colon tissues as evidenced by necrotic mucosal cells, inflammatory cell infiltration, submucosa edema, the disappearance of crypts, gland structures, and goblet cells. These clinical symptoms and pathological alterations were significantly improved by 23-HBA suggesting that 23-HBA has a protective effect on UC.

Highly expressed COX-2 and iNOS play important roles in the initiation and propagation of the inflammatory cascade [21,22]. COX-2 is an enzyme that could catalyze arachidonic acid into prostaglandin H2 (PGH2) and further into PGE2 by prostaglandin synthase [23]. Increased iNOS expression and a high amount of NO production were involved in UC pathogenesis [24]. Here, 23-HBA significantly inhibited DSS-induced COX-2 and iNOS expression using western blotting analysis, which was further confirmed by immunohistochemistry. The inhibitory effect of 23-HBA was further confirmed in LPS-stimulated RAW264.7 cells. A study showed that AB4 inhibited COX-2 and iNOS expression in LPS-stimulated THP-1 cells and acute lung injury (ALI) mouse models [25] but with higher concentrations. Thus, both 23-HBA and AB4 could inhibit COX-2 and iNOS.

Oxidative stress and inflammatory cytokines, such as TNFα, IL-6, IL-1β, IL-10, etc play important roles in the initiation and development of UC [26-28]. MDA and MPO are oxidative stress biomarkers whereas SOD is a critical antioxidant enzyme. The inhibitory effect of 23-HBA on MDA, MPO, and ROS indicated that it has an anti-oxidant effect, directly or indirectly. Similar to the inhibitory effect of AB4 in DSS-induced colitis [14], 23-HBA showed a significant anti-inflammatory effect by suppressing the secretion of IL-1β and IL-6 in colon tissues. Interestingly, it also promoted the secretion of IL-10, an anti-inflammatory cytokine. Thus, 23-HBA may disturb the balance of pro- and anti-inflammatory cytokines in the UC model.

The activation of the NF-κB pathway which includes p-IKKα/β, p-IκBα, NF-κB p65, p50, etc, was one of the key regulators in UC and colorectal cancer. NF-κB pathway activation increases the expression of various pro-inflammatory genes, such as TNFα, IL-6, IL-1β, etc. Furthermore, iNOS and COX-2 expressions were also regulated by the NF-κB pathway. Documented data showed that the NF-κB pathway strongly influences the course of mucosal inflammation [29-31]. Here, for the first time, we found that 23-HBA potently inhibited the NF-κB pathway in colitis colon tissues and LPS-stimulated RAW 264.7 cells. The canonical pathway of NF-κB activation by pathologic stimuli is the formation of a p65:p50 heterodimer. Thus, the NF-κB p65 has been regarded as a promising target for drug discovery [32]. We previously reported that two natural compounds isobavachalcone and neferine suppressed DSS-induced colitis and colitis-associated colorectal cancer by inhibiting NF-κB p65 [15,33]. Here, the inhibitory effect of 23-HBA on NF-κB p65 and p-p65 was confirmed by western blotting, immunohistochemistry, and immunofluorescence. Furthermore, this inhibition may be indirect and mediated by its regulation of IKKα and/or IκBα, two upstream regulators of NF-κB p65. Anyway, the activation of the NF-κB pathway was significantly suppressed by 23-HBA. Given that many natural compounds were potent inhibitors of NF-κB [34], p65 might be the potential target for 23-HBA, which needs further investigation.

The protective effect of AB4, a 23-HBA analog, on DSS-induced UC involved the inhibition of several pathways, such as TLR4, NF-κB, and MAPK [14]. Furthermore, TLR4 was reported to be involved in the protective effect of AB4 against ALI [25]. Here, LPS-induced TLR4 expression in RAW264.7 cells and expression of MyD88, a key mediator of TLR4 signaling, in colon tissues, were significantly suppressed by 23-HBA. These results suggested that 23-HBA shared similarity with AB4 and might affect TLR4 signaling. However, the exact role of TLR4 needs further investigation. The MAPK signaling participated in the protective effect of AB4 in colitis. Due to its downstream role, the effect of 23-HBA on MAPK signaling was not determined in this study, which could be explored in future studies.

In conclusion, our data showed that a natural compound, 23-HBA alleviated experimental UC triggered by DSS in mice and inhibited inflammation induced by LPS in macrophages. These inhibitory effects of 23-HBA might be related to its inhibition of the NF-κB signaling pathway.

Data Availability Statement: The datasets generated during and/or analysed during the current study are available from the corresponding author on reasonable request.

Conflicts of Interest: The authors have declared that there is no conflict of interest.

References

1. Ungaro R.; Mehandru S.; Allen P.B.; et al. Ulcerative colitis. *The Lancet*, **2017**, *389*(10080): 1756-1770.
2. Ng S.C.; Tang W.; Ching J.Y.; et al. Incidence and phenotype of inflammatory bowel disease based on results from the Asia-pacific Crohn's and colitis epidemiology study. *Gastroenterology*, **2013**, *145*(1): 158-165 e152.
3. Park J.A.-O.;Cheon J.A.-O. Incidence and Prevalence of Inflammatory Bowel Disease across Asia. *Yonsei Med. J.* **2021**, *62*(2): 99-108.
4. Hendrickson B.A.; Gokhale R.;Cho J.H. Clinical aspects and pathophysiology of inflammatory bowel disease. *Clin Microbiol Rev*, **2002**, *15*(1): 79-94.
5. Ordás I.; Eckmann L.; Talamini M.; et al. Ulcerative colitis. *The Lancet*, **2012**, *380*(9853): 1606-1619.
6. Zhou J.; Lai W.; Yang W.; et al. BLT1 in dendritic cells promotes Th1/Th17 differentiation and its deficiency ameliorates TNBS-induced colitis. *Cell. Mol. Immunol*, **2018**, *15*(12): 1047-1056.
7. Miao Z.; Chen L.; Feng H.; et al. Baitouweng Decoction Ameliorates Ulcerative Colitis in Mice Partially Attributed to Regulating Th17/Treg Balance and Restoring Intestinal Epithelial Barrier. *Front. Pharmacol.*, **2020**, *11*: 531117.
8. Xuan-Qing C.; Xiang-Yu L. V.; Shi-Jia L. I. U. Baitouweng decoction alleviates dextran sulfate sodium-induced ulcerative colitis by regulating intestinal microbiota and the IL-6/STAT3 signaling pathway. *J. Ethnopharmacol.*, **2021**, *265*: 113357.
9. Wang X.; Xu L.; Wang T.; et al. Pulsatilla decoction alleviates colitis by enhancing autophagy and regulating PI3KAktmTORC1 signaling pathway. *Mol. Med. Rep.*, **2022**, *25*(3).
10. Li Y.H.; Zou M.; Han Q.; et al. Therapeutic potential of triterpenoid saponin anemoside B4 from Pulsatilla chinensis. *Pharmacol. Res.*, **2020**, *160*: 105079.
11. Ye B.;Ji Z.N. 23-hydroxybetulinic acid-induced HL-60 cell autophagic apoptosis and its molecular mechanism. *Nat. Prod. Res.*, **2012**, *26*(11): 1063-1068.
12. Ji Z.N.; Ye W.C.; Liu G.G.; et al. 23-Hydroxybetulinic acid-mediated apoptosis is accompanied by decreases in bcl-2 expression and telomerase activity in HL-60 Cells. *Life Sci.*, **2002**, *72*(1): 1-9.
13. Zhou F.; Hao G.; Zhang J.; et al. Protective effect of 23-hydroxybetulinic acid on doxorubicin-induced cardiotoxicity: a correlation with the inhibition of carbonyl reductase-mediated metabolism. *Br. J. Pharmacol.*, **2015**, *172*(23): 5690-5703.
14. Ma H.; Zhou M.; Duan W.; et al. Anemoside B4 prevents acute ulcerative colitis through inhibiting of TLR4/NF-κB/MAPK signaling pathway. *Int. Immunopharmacol.*, **2020**, *87*: 106794.
15. Wirtz S.; Popp V.; Kindermann M.; et al. Chemically induced mouse models of acute and chronic intestinal inflammation. *Nat. Protoc.*, **2017**, *12*(7): 1295-1309.
16. Zhou Y.; Zhong B.; Min X.; et al. Therapeutic potential of isobavachalcone, a natural flavonoid, in murine experimental colitis by inhibiting NF-κB p65. *Phytother. Res.*, **2021**, *35*(10): 5861-5870.
17. Wu X.; Guo Y.; Min X.; et al. Neferine, a Bisbenzylisoquinoline Alkaloid, Ameliorates Dextran Sulfate Sodium-Induced Ulcerative Colitis. *Am. J. Chin. Med.*, **2018**, *46*(6): 1263-1279.
18. Guo Y.; Wu X.; Wu Q.; et al. Dihydrotanshinone I, a natural product, ameliorates DSS-induced experimental ulcerative colitis in mice. *Toxicol. Appl. Pharmacol.*, **2018**, *344*: 35-45.
19. Eichele D.D.;Kharbanda K.K. Dextran sodium sulfate colitis murine model: An indispensable tool for advancing our understanding of inflammatory bowel diseases pathogenesis. *World J. Gastroenterol.*, **2017**, *23*(33): 6016-6029.
20. Perše M.; Cerar A. Dextran sodium sulphate colitis mouse model: traps and tricks. *J. Biomed. Biotechnol.*, **2012**, *2012*: 718617.
21. Chen L.; Teng H.; Fang T.; et al. Agrimonolide from Agrimonia pilosa suppresses inflammatory responses through down-regulation of COX-2/iNOS and inactivation of NF-kappaB in lipopolysaccharide-stimulated macrophages. *Phytomedicine*, **2016**, *23*(8): 846-855.
22. Lee J. S.; Kim H. S.; Hahm K. B.; et al. Effects of Genetic and Pharmacologic Inhibition of COX-2 on Colitis-associated Carcinogenesis in Mice. *J. Cancer Prev.*, **2020**, *25*(1): 27-37.
23. Kotha Subbaramaiah N. T., John T. Ramonetti, Ruriko Araki, Bethany De Vito, Babette B. Weksler, and Andrew J. Dannenberg. Transcription of Cyclooxygenase-2 Is Enhanced in Transformed Mammary Epithelial Cells. *Cancer Res.*, **1996**, *56*(19): 4424-4429.
24. Middleton S.J.; Shorthouse M.;Hunter J.O. Increased nitric oxide synthesis in ulcerative colitis. *The Lancet*, **1993**, *341*(8843): 465-466.
25. Yuan R.; He J.; Huang L.; et al. Anemoside B4 Protects against Acute Lung Injury by Attenuating Inflammation through Blocking NLRP3 Inflammasome Activation and TLR4 Dimerization. *J. Immunol. Res.*, **2020**, *2020*: 7502301.
26. Kaur A.; Goggolidou P. Ulcerative colitis: understanding its cellular pathology could provide insights into novel therapies. *J. Inflamm. (Lond)*, **2020**, *17*: 15.
27. Nakase H.; Sato N.; Mizuno N.; et al. The influence of cytokines on the complex pathology of ulcerative colitis. *Autoimmun. Rev.*, **2022**, *21*(3): 103017.
28. Pereira C.; Grácio D.; Teixeira J.P.; et al. Oxidative Stress and DNA Damage: Implications in Inflammatory Bowel

Disease. *Inflamm. Bowel. Dis.*, **2015**, *21*(10): 2403-2417.

29. Atreya I.; Atreya R.;Neurath M.F. NF-kappaB in inflammatory bowel disease. *J Intern Med*, **2008**, *263*(6): 591-596.

30. DiDonato J.A.; Mercurio F.;Karin M. NF-κB and the link between inflammation and cancer. *Immunol. Rev.*, **2012**, *246*(1): 379-400.

31. Surh Y. J.; Chun K. S.; Cha H. H.; et al. Molecular mechanisms underlying chemopreventive activities of anti-inflammatory phytochemicals: down-regulation of COX-2 and iNOS through suppression of NF-kappa B activation. *Mutat. Res.*, **2001**, *480-481*: 243-268.

32. Giridharan S.;Srinivasan M. Mechanisms of NF-κB p65 and strategies for therapeutic manipulation. *J. Inflamm. Res.*, **2018**, *11*: 407-419.

33. Zhou Y.; Xiang S.; Zheng H.; et al. Neferine Suppresses Experimental Colitis-Associated Colorectal Cancer by Inhibition of NF-[Formula: see text]B p65 and STAT3. *Am. J. Chin. Med.*, **2022**, *50*(5): 1387-1400.

34. Nam N.H. Naturally occurring NF-kappaB inhibitors. *Mini. Rev. Med. Chem.*, **2006**, *6*(8): 945-951.

Publisher's Note: Scilight stays neutral with regard to jurisdictional claims in published maps and institutional affiliations.